THE BELL SYSTEM TECHNICAL JOURNAL
Vol. 57, No. 7, September 1978
Printed in U.S.A.

Adaptive Equalization of Channel Nonlinearities in QAM Data Transmission Systems

By D. D. FALCONER

(Manuscript received August 23, 1977)

Within the population of voiceband telephone channels, few channel characteristics are as pervasive in their impairment of high-speed data communication as nonlinear distortion, which cannot be removed or equalized in the receiver as easily as can linear distortion. The purpose of this paper is to report on an investigation of a QAM receiver incorporating adaptive equalization of nonlinearities as well as adaptive decision feedback equalization and data-aided carrier recovery for mitigation of linear distortion and phase jitter, respectively. Nonlinearities are equalized by adding to the received in-phase and quadrature signals a weighted sum of nonlinear functionals of the received signal and of modulated previous receiver decisions. The choice of nonlinear terms in the sum is based on a channel model incorporating quadratic and cubic nonlinearities as well as linear dispersive elements. The adjustment of the weighting, or tap, coefficients for the various terms is based on a gradient algorithm, as is the adjustment of the linear tap coefficients and the carrier phase reference. The feasibility of nonlinearity equalization on real voiceband channels was confirmed in a test in which recorded 9600-bps QAM signals, received from a worse-than-average set of 17 voiceband telephone channels, were processed by a computer-simulated version of the proposed receiver (termed the NL receiver). The observed error rates for all channels were lower, in some cases by several orders of magnitude, than those achieved by computer-simulated versions of the linear receiver and of a decision feedback equalization receiver (termed the DFE receiver).

I. INTRODUCTION

The prevalence of nonlinearities and their distorting effect on high-speed data transmission over voiceband telephone channels has long been recognized.[1] The effect of nonlinear distortion on linearly modulated data signals is to introduce nonlinear intersymbol interference and

reduce the margin against noise. For data rates above 4800 bps, nonlinear distortion is the dominant impairment on many voiceband telephone channels. Experimental studies have measured nonlinear distortion and related the observed error rates for specific modulation formats to this and other measured impairments.[2,3] Estimation of performance for data transmission in the presence of nonlinearities can be carried out[4] but gives little insight into the problem of receiver optimization, except for certain simple nonlinear channel models.[5]

Recognizing that nonlinearities in transmission channels generally coexist with linear elements such as filters, one is led to consider a general nonlinear receiver structure, based on a Volterra or Wiener kernel characterization[6] of a general nonlinear system such as that proposed in Refs. 5, 7, and 8, the latter in connection with adaptive echo cancellation. In the present work, we extend this approach by generalizing the structure of a passband decision feedback equalizer, previously studied in connection with linear channel distortion,[9] to process nonlinear as well as linear functionals of the incoming signal and prior decisions.*

The new receiver structure is based on a model of a passband channel with quadratic and cubic nonlinearities, as well as linear filters. We report on the simulation of the new receiver and on comparisons of its performance with two other previously simulated 9600-bps QAM receivers on a worse-than-average set of voiceband telephone channels. The new receiver is referred to as the NL receiver. The other two receivers, designated LE (linear equalization) and DFE (decision feedback equalization), are not designed to compensate for channel nonlinearities. Their performance is compared over the same set of voiceband telephone channels in Ref. 9. The simulated LE receiver is described in Ref. 10.

II. SUMMARY OF THE MAJOR RESULTS

The relative performances of the three simulated receivers on the same set of recorded, received, 9600-bps data signals are briefly summarized as follows: On every channel, the NL receiver yielded a lower error probability than the other two receivers. For 13 out of the 17 channels, the improvement in error rate was equal to or better than about an order of magnitude. Another gauge of the degree of improvement offered by the NL receiver is the fact that it increased the number of channels yielding a better-than-10^{-4} error rate from 8 to 15. On one channel, whose major impairment was second harmonic distortion, the NL re-

* Figure 3a summarizes the structure of the nonlinearity-equalizing receiver.

ceiver's error rate bested that of the DFE and LE receiver by over four orders of magnitude. Figure 5 is a bar graph summarizing the error rate comparisons.

The apparent attractiveness of the NL receiver structure is, however, tempered by its greater complexity. A large number of nonlinear tap coefficients is necessary to account and compensate for the dispersive nonlinear effects typically encountered on voiceband channels. In the simulations summarized above, the LE and DFE receivers each had 32 complex tap coefficients, but the NL receiver was, roughly speaking, comparable in complexity to an LE receiver with 134 complex tap coefficients. Reducing the number of coefficients in the NL receiver lowered its performance margin over the other receivers. Furthermore, the best allocation of a fixed number of tap coefficients varied from one channel to another. These points are explored more fully in later sections.

In spite of the greater complexity of the NL receiver structure, the performance comparison of the three receivers does indicate the importance of alleviating nonlinear distortion for high-speed data transmission.

III. THE CHANNEL MODEL

Obviously, the effect of channel nonlinearities on a passband QAM data signal must be understood before a compensating receiver structure can be suggested. A general representation of a bandlimited QAM signal is as the real part of a complex waveform:

$$x(t) = \mathrm{Re}\left[e^{j2\pi f_c t} \sum_n A(n)F(t - nT) \right], \tag{1}$$

where $j = \sqrt{-1}$, f_c is the carrier frequency, $A(n)$ is a quantized complex number representing the information symbol in the nth symbol interval (for example, in the case of four-level QAM, the real and imaginary parts of $A(n)$ assume one of the four possible values $\pm 1, \pm 3$), T is the reciprocal of the baud, and $F(t)$ is a complex pulse waveform.

In the case of QAM signals, extraction of the information symbols represented by the complex number $A(n)$ requires two receiver outputs, which are derived by appropriate operations on both the received passband signal and on its quadrature version, or Hilbert transform. A phase-splitting filter is used to obtain both in-phase and quadrature versions of a voiceband data signal.

The complex waveform

$$X(t) = e^{j2\pi f_c t} \sum_n A(n)F(t - nT) \tag{2}$$

is assumed analytic;[11] that is, its spectrum is twice the Fourier transform of $x(t)$ for positive frequencies and is zero elsewhere. Furthermore, we assume the spectrum is limited on the high side to frequency $2f_c$. Note that the Fourier transform $\mathcal{F}(f)$ of the complex pulse $F(t)$ is not necessarily symmetric about $f = 0$, but it is assumed to be strictly band-limited to $-f_c < f < f_c$. The Nyquist frequency is $1/2T$ Hz. Figure 1 shows a sketch of $\mathcal{F}(f)$ and of $\mathcal{F}(f - f_c)$, which is the Fourier transform of $e^{j2\pi f_c t}F(t)$.

The notion of analytic signals is a notational convenience. The Hilbert transform, or quadrature version of a signal $u(t)$, is a linear functional of $u(t)$:

$$\check{u}(t) = \frac{1}{\pi}\int_{-\infty}^{\infty} \frac{u(\tau)}{t - \tau}\, d\tau.$$

It can be shown that there is a unique analytic signal whose real part is $u(t)$, and that $\check{u}(t)$ is then just the imaginary part of the analytic signal. Conversely, any analytic signal comprises some real signal plus j times its Hilbert transform. Since QAM systems operate on both in-phase and quadrature versions of signals, they are most conveniently represented by means of analytic signals.

The nonlinear receiver structure will be based on the simple nonlinear channel model shown in Fig. 2, using the notation of analytic signals. Filters 1, 2, and 3 are passband with the same bandwidth as the transmitted data signal. The filters may include the receiver's input filter as well as the linear response of the channel. The quadratic and cubic memoryless nonlinearities with attenuated outputs account for second

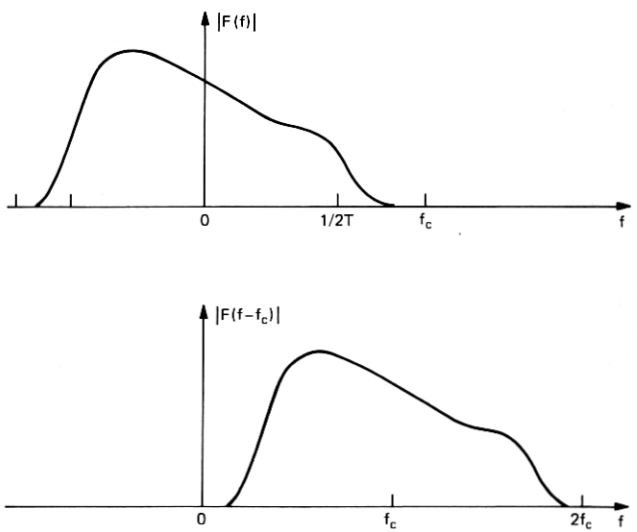

Fig. 1—Fourier transforms of $|F(f)|$ and $|F(f - c)|$.

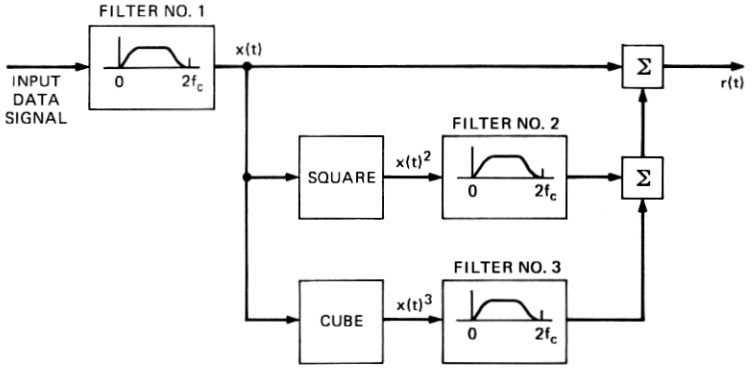

Fig. 2—Model of a nonlinear channel.

and third harmonic distortion, respectively. Additional impairments not shown in Fig. 2 are phase jitter, which implies multiplication of the complex received signal by $e^{j\phi(t)}$, and additive noise.

The result of passing the transmitted waveform through the linear portion of the channel (filter 1) is an analytic waveform in the form of eq. (2). A passband linear[10,12] equalizer (LE) can be used to minimize the mean squared error between its output, sampled at times nT, and a reference $A(n)e^{j(2\pi f_c nT+\hat{\theta}(n))}$, which is the complex information symbol modulated to passband with a receiver phase reference $\hat{\theta}(n)$. In a linear receiver, the passband equalizer output is demodulated [multiplied by $e^{-j(2\pi f_c nT+\hat{\theta}(n))}$] and then quantized to yield a decision $\hat{A}(n)$. A passband equalizer configuration which is theoretically more effective in combatting linear intersymbol interference is the passband DFE, described in Ref. 9.

To motivate a receiver structure which is appropriate for nonlinear distortion as well as linear distortion, we must consider the analytic signals emanating from the quadratic and cubic path elements of Fig. 2.

It is shown in the appendix that the analytic signal output from the model of Fig. 2 is of the form

$$R(t) = U_0(t) + e^{j2\pi f_c t}U_{11}(t) + e^{-j2\pi f_c t}U_{12}(t) + e^{j4\pi f_c t}U_2(t) + e^{j6\pi f_c t}U_3(t), \quad (3a)$$

where

$$U_0(t) = \sum_{n_1,n_2} A(n_1)A(n_2)^* G_0(t - n_1T, t - n_2T) \quad (3b)$$

$$U_{11}(t) = \sum_n A(n)F(t - nT) + \sum_{n_1,n_2,n_3} A(n_1)A(n_2)A(n_3)^* G_{11}(t - n_1T, t - n_2T, t - n_3T) \quad (3c)$$

$$U_{12}(t) = \sum_{n_1,n_2,n_3} A(n_1)^* A(n_2)^* A(n_3) G_{12}(t - n_1T, t - n_2T, t - n_3T) \tag{3d}$$

$$U_2(t) = \sum_{n_1,n_2} A(n_1)A(n_2)G_2(t - n_1T, t - n_2T) \tag{3e}$$

$$U_3(t) = \sum_{n_1,n_2,n_3} A(n_1)A(n_2)A(n_3)G_3(t - n_1T, t - n_2T, t - n_3T), \tag{3f}$$

where asterisks denote complex conjugates.

The various U terms are seen to be linear combinations of products of complex information symbols $A(n)$, $A(n_1)A(n_2)$, $A(n_1)A(n_2)A(n_3)^*$, etc. Each modulates a harmonic of the carrier wave. The term $e^{j2\pi f_c t}$-$U_{11}(t)$ includes the linear response of the channel to the data signal and also a component resulting from cubic distortion. The terms $U_0(t)$ and $U_2(t)$ result from the quadratic nonlinearity and the terms $U_{12}(t)$ and $U_3(t)$ result from the cubic nonlinearity. Additional terms would, of course, result from the assumption of additional nonlinear elements in the model of Fig. 2. The generalization of expression (3) to an infinite power series would be a complex passband version of a Volterra expansion.

IV. THE NONLINEAR RECEIVER STRUCTURE

The receiver structure to be studied here includes the passband QAM decision feedback equalizer discussed in Ref. 9, plus nonlinear processing suggested by the set of eqs. (3). Let $Y(n)$ be the receiver's complex output at time $t = nT$. This output is quantized to form the decision $\hat{A}(n)$, which equals the original transmitted symbol $A(n)$ if no error occurred. Let the demodulator's phase reference at time nT be $\hat{\theta}(n)$. Let $\{W_k^{(1)}\}_{k=-N}^{N}$ and $\{B_k^{(1)}\}_{k=1}^{M}$ be the complex linear forward and feedback tap coefficients respectively, and let $\{R(n)\}$ be the complex receiver input, sampled at times nT. Then

$$Y(n) = e^{-j(2\pi f_c nT + \hat{\theta}(n))} \sum_{k=-N}^{N} W_k^{(1)*} R(n-k) - \sum_{k=1}^{M} B_k^{(1)*} \hat{A}(n-k) + Y_{NL}(n) e^{-j(2\pi f_c nT + \hat{\theta}(n))}, \tag{4a}$$

where $Y_{NL}(n)$ consists of nonlinear functions of $\{R(k)\}$ and $\{\hat{A}(k)\}_{k<n}$.

The linear part of eq. (4a) implies a demodulated linear combination of $2N + 1$ receiver input samples minus a linear combination of M previous decisions.

The nonlinear term $Y_{NL}(n)$ is heuristically suggested by expression (3) in the following way: (*i*) Assume that at time nT the previous receiver decisions $\hat{A}(k) = A(k)(k < n)$ and that they are available to form the

nonlinear feedback terms. (*ii*) In any terms of expression (3) involving decisions $\hat{A}(k)$ not yet made at time $n(k \geq n)$, replace $\hat{A}(k)e^{j2\pi f_c kT+\hat{\theta}(k)}$ by $R(k)$ to form the forward nonlinear terms. The resulting expression is

$$
\begin{aligned}
Y_{NL}(n) = & \sum_{k_1,k_2} W^{(0)*}_{k_1k_2} R(n-k_1)R(n-k_2)^* \\
& + \sum_{k_1,k_2,k_3} W^{(11)*}_{k_1,k_2,k_3} R(n-k_1)R(n-k_2)R(n-k_3)^* \\
& + \sum_{k_1,k_2,k_3} W^{(12)*}_{k_1,k_2,k_3} R(n-k_1)^*R(n-k_2)^*R(n-k_3) \\
& + \sum_{k_1,k_2} W^{(2)*}_{k_1,k_2} R(n-k_1)R(n-k_2) \\
& + \sum_{k_1,k_2,k_3} W^{(3)*}_{k_1,k_2,k_3} R(n-k_1)R(n-k_2)R(n-k_3) \\
& - e^{j\hat{\theta}(n)} \sum_{\substack{k_1,k_2 \\ \geq 1}} B^{(0)*}_{k_1,k_2} \hat{A}(n-k_1)\hat{A}(n-k_2)^* \\
& - e^{j(2\pi f_c nT+\hat{\theta}(n))} \sum_{\substack{k_1,k_2,k_3 \\ \geq 1}} B^{(11)*}_{k_1,k_2,k_3} \hat{A}(n-k_1)\hat{A}(n-k_2)\hat{A}(n-k_3)^* \\
& - e^{-j(2\pi f_c nT-\hat{\theta}(n))} \sum_{\substack{k_1,k_2,k_3 \\ \geq 1}} B^{(12)*}_{k_1,k_2,k_3} \hat{A}(n-k_1)^*\hat{A}(n-k_2)^*\hat{A}(n-k) \\
& - e^{j(4\pi f_c nT+\hat{\theta}(n))} \sum_{\substack{k_1,k_2 \\ \geq 1}} B^{(2)*}_{k_1,k_2} \hat{A}(n-k_1)\hat{A}(n-k_2) \\
& - e^{j(6\pi f_c nT+\hat{\theta}(n))} \sum_{\substack{k_1,k_2,k_3 \\ \geq 1}} B^{(3)*}_{k_1,k_2,k_3} \\
& \times \hat{A}(n-k_1)\hat{A}(n-k_2)\hat{A}(n-k_3). \quad \text{(4b)}
\end{aligned}
$$

The formidable-looking expression (4b) is a linear combination of products of receiver inputs and their complex conjugates, minus a linear combination of products of previous decisions and their complex conjugates, modulated by appropriate harmonics of the carrier.

Figures 3a and 3b are block diagrams of the NL receiver. The cross-hatched boxes in Figure 3a show the nonlinear processing that has been added to the basic decision feedback equalization structure described in an earlier paper.[9]

V. ADAPTATION OF RECEIVER PARAMETERS

As in the linear and decision feedback equalization receivers, the parameters $\{W\}$, $\{B\}$ and $\hat{\theta}$ are adjusted in an estimated gradient algorithm to minimize the average value of the squared error magnitude $|E(n)|^2$ defined by

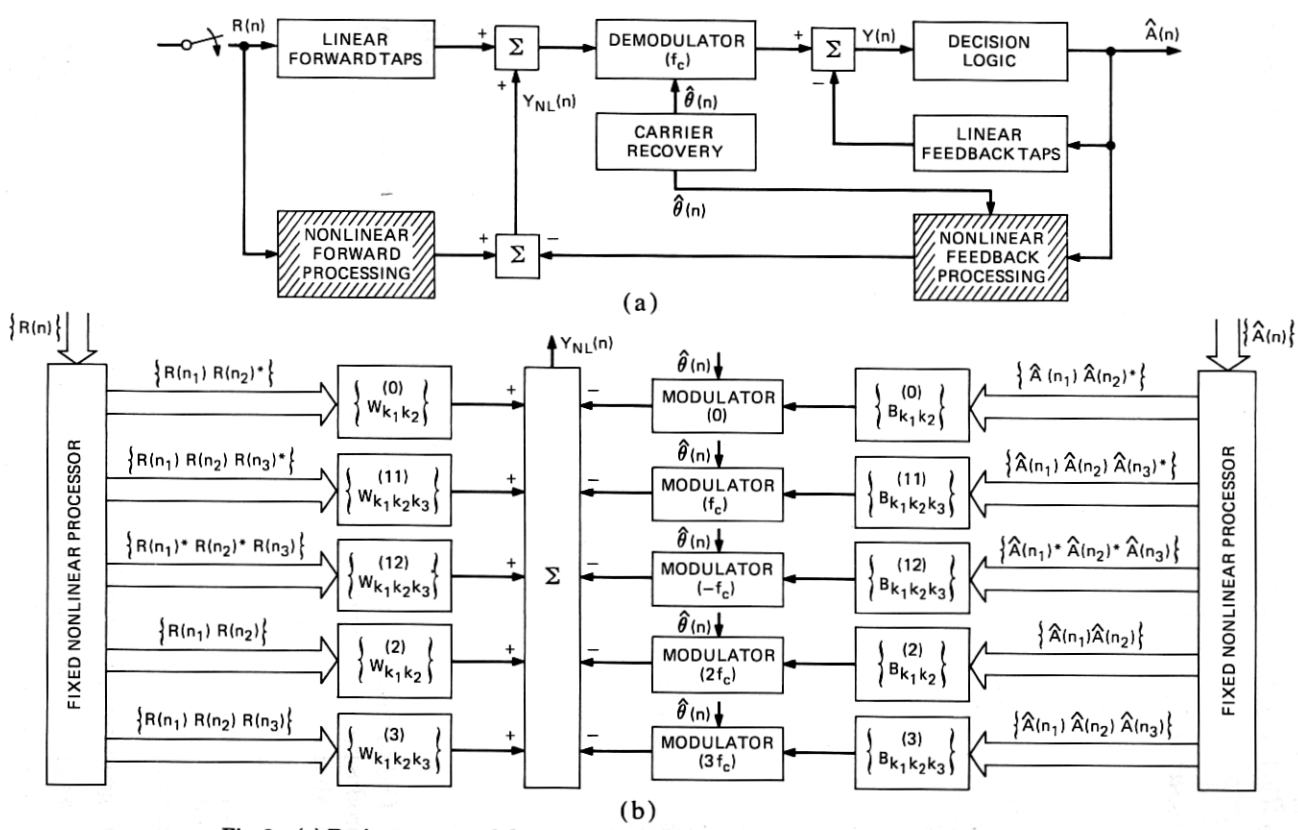

Fig. 3—(a) Basic structure of the NL receiver. (b) Details of the nonlinear signal processing.

$$E(n) \equiv Y(n) - A(n). \tag{5}$$

The error $E(n)$, as in the previous receivers, is a *linear* function of the parameters $\{W\}$ and $\{B\}$; consequently, the expression for $|E(n)|^2$ is convex in these parameters.

In writing the updating equations for the $\{W(n)\}$ and $\{B(n)\}$ coefficients and for $\hat{\theta}(n)$ in the nth symbol interval, it is convenient to use the symbol $\epsilon(n)$ to denote the *observed passband* error after the decision $A(n)$ has been made:

$$\epsilon(n) = [Y(n) - \hat{A}(n)]e^{j(2\pi f_c nT + \hat{\theta}(n))}; \tag{6a}$$

thus, if $\hat{A}(n) = A(n)$, $|E(n)|^2 = |\epsilon(n)|^2$, and the expression for the gradient of $|\epsilon(n)|^2$ with respect to each parameter determines an adjustment algorithm for that parameter. The adjustment equation for $\hat{\theta}(n)$ is as follows:

$$\hat{\theta}(n+1) = \hat{\theta}(n) - \frac{\alpha Im[\epsilon(n)^* Z(n)]}{|\hat{A}(n)|^2}, \tag{6b}$$

where
$$\begin{aligned} Z(n) = \sum_{k=-N}^{N} W_k^{(1)*} R(n-k) \\ + \sum_{k_1,k_2} W_{k_1,k_2}^{(0)*} R(n-k_1)R(n-k_2)^* \\ + \sum_{k_1,k_2,k_3} W_{k_1,k_2,k_3}^{(11)*} R(n-k_1)R(n-k_2)R(n-k_3)^* \\ + \sum_{k_1,k_2,k_3} W_{k_1,k_2,k_3}^{(12)*} R(n-k_1)^* R(n-k_2)^* R(n-k_3) \\ + \sum_{k_1,k_2} W_{k_1,k_2}^{(2)*} R(n-k_1)R(n-k_2) \\ + \sum_{k_1,k_2,k_3} W_{k_1,k_2,k_3}^{(3)*} R(n-k_1)R(n-k_2)R(n-k_3) \end{aligned} \tag{6c}$$

is the sum of all the forward terms comprising $Y(n)$. The adjustment equations for the $\{W\}$ and $\{B\}$ coefficients are as follows:

$$W_{k_1,k_2}^{(0)}(n+1) = W_{k_1,k_2}^{(0)}(n) - \beta_0 \epsilon(n)^* R(n-k_1)R(n-k_2)^* \tag{6d}$$

$$W_k^{(1)}(n+1) = W_k^{(1)}(n) - \beta_1 \epsilon(n)^* R(n-k) \tag{6e}$$

$$W_{k_1,k_2,k_2}^{(11)}(n+1) = W_{k_1,k_2,k_3}^{(11)}(n) - \beta_{11}\epsilon(n)^* R(n-k_1) \cdot R(n-k_2)R(n-k_3)^* \tag{6f}$$

$$W_{k_1,k_2,k_3}^{(12)}(n+1) = W_{k_1,k_2,k_3}^{(12)}(n) - \beta_{12}\epsilon(n)^* R(n-k_1)^* \cdot R(n-k_2)^* R(n-k_3) \tag{6g}$$

$$W_{k_1,k_2}^{(2)}(n+1) = W_{k_1,k_2}^{(2)}(n) - \beta_2 \epsilon(n)^* R(n-k_1)R(n-k_2) \tag{6h}$$

$$W_{k_1,k_2,k_3}^{(3)}(n+1) = W_{k_1,k_2,k_3}^{(3)}(n) - \beta_3 \epsilon(n)^* R(n-k_1) \cdot R(n-k_2)R(n-k_3) \tag{6i}$$

$$B^{(0)}_{k_1,k_2}(n+1) = B^{(0)}_{k_1,k_2}(n) + \gamma_0 \epsilon(n)^* \hat{A}(n-k_1)\hat{A}(n-k_2)^* e^{j\hat{\theta}(n)} \quad (6j)$$

$$B^{(1)}_{k}(n+1) = B^{(1)}_{k}(n) + \gamma_1 \epsilon(n)^* A(n-k) e^{j(2\pi f_c nT + \theta(n))} \quad (6k)$$

$$B^{(11)}_{k_1,k_2,k_3}(n+1) = B^{(11)}_{k_1,k_2,k_3}(n) + \gamma_{11} \epsilon(n)^* \hat{A}(n-k_1)\hat{A}(n-k_2)\hat{A}(n-k_3)^* e^{j(2\pi f_c nT + \hat{\theta}(n))} \quad (6l)$$

$$B^{(12)}_{k_1,k_2,k_3}(n+1) = B^{(12)}_{k_1,k_2,k_3}(n) + \gamma_{12} \epsilon(n)^* \hat{A}(n-k_1)^* \hat{A}(n-k_2)^* \hat{A}(n-k_3) e^{-j(2\pi f_c nT + \hat{\theta}(n))} \quad (6m)$$

$$B^{(2)}_{k_1,k_2}(n+1) = B^{(2)}_{k_1,k_2}(n) + \gamma_2 \epsilon(n)^* \hat{A}(n-k_1) \cdot \hat{A}(n-k_2) e^{j(4\pi f_c nT + \hat{\theta}(n))} \quad (6n)$$

$$B^{(3)}_{k_1,k_2,k_3}(n+1) = B^{(3)}_{k_1,k_2,k_3}(n) + \gamma_3 \epsilon(n)^* \hat{A}(n-k_1)\hat{A}(n-k_2)\hat{A}(n-k_3) e^{j(6\pi f_c nT + \hat{\theta}(n))}. \quad (6o)$$

The set of eqs. (4) through (6) defines the structure of the nonlinear QAM receiver that has been simulated. The α, β, and γ parameters are positive constants, chosen to ensure reasonably fast convergence and stability in the presence of noise. To enable compensation of rapidly varying phase jitter, the phase tracking constant α was set to the relatively large value of 0.4. The other constants chosen were:

$$\beta_1 = \gamma_1 = 0.001, \beta_0 = \beta_2 = \gamma_0 = \gamma_2 = 0.75 \times 10^{-5},$$
$$\beta_{11} = \beta_{12} = \beta_3 = \gamma_{11} = \gamma_{12} = \gamma_3 = 10^{-6}.$$

A judicious choice must be made for the range of coefficient indices k_1, k_2, and k_3 in the nonlinear terms making up $Y_{NL}(n)$, if the total number of $\{W\}$ and $\{B\}$ coefficients is to be reasonable, say on the order of 100. Obviously, the best choice of indices for a fixed number of taps depends on the channel. Trial and error (by no means exhaustive) of various sets of indices used in simulations on several voiceband channels led to the choice of terms shown in Table I. There are 73 "forward" tap coefficients $\{W\}$, of which 22 are linear, and 61 "feedback" tap coefficients $\{B\}$, of which 10 are linear. Note that the nonlinear forward tap indices are confined to the range $-1 \leq k \leq 1$ and the nonlinear feedback tap indices have been confined to the range $1 \leq k \leq 3$.

VI. THE SIMULATIONS

The nonlinear QAM receiver structure described in the previous section was simulated on an IBM 360 computer to process recorded 9600-bps QAM data signals that had been received from 17 voiceband telephone channels. The simulation effort was an extension of that described for linear and decision feedback QAM receivers in Refs. 3 and 9, respectively. The set of recorded QAM signals was the same, permitting the performance of all three receiver types to be compared under identical con-

Table I — Index terms used in voiceband simulations

Terms	Indices k_1	k_2	k_3	Terms	Indices k_1	k_2	k_3
$W^{(0)}_{k1,k2}$	−1	−1		$B^{(0)}_{k1,k2}$	1	1	
	0	0			2	2	
	1	1			3	3	
	−1	0			2	1	
	0	−1			1	2	
	0	1			3	2	
	1	0			2	3	
	−1	1			3	1	
	1	−1			1	3	
$W^{(1)}_{k1}$ (Linear) terms −12 to 9 inclusive				$B^{(1)}_{k1}$ (Linear) terms 1 to 10 inclusive			
$W^{(11)}_{k1,k2,k3}$				$B^{(11)}_{k1,k2,k3}$ and			
and $W^{(12)}_{k1,k2,k3}$	−1	−1	−1	$B^{(12)}_{k1,k2,k3}$	1	1	1
	0	0	0		2	2	2
	1	1	1		3	3	3
	−1	−1	0		1	1	2
	−1	0	−1		1	2	1
	0	0	−1		2	2	1
	0	−1	0		2	1	2
	0	0	1		2	2	3
	0	1	0		2	3	2
	1	1	0		3	3	2
	1	0	1		3	2	3
	−1	0	1		1	2	3
	0	1	−1		2	3	1
	−1	1	0		1	3	2
$W^{(2)}_{k1,k2}$	−1	−1		$B^{(2)}_{k1,k2}$	1	1	
	−1	0			2	2	
	0	0			3	3	
	1	1			1	2	
	0	1			2	3	
	−1	1			1	3	
$W^{(3)}_{k1,k2,k3}$	−1	−1	−1	$B^{(3)}_{k1,k2,k3}$	1	1	1
	0	0	0		2	2	2
	−1	−1	0		1	1	2
	0	0	−1		2	2	1
	1	1	1		3	3	3
	0	0	1		2	2	3
	1	1	0		3	3	2
	−1	0	1		1	2	3

ditions. The set of 17 channels could be described as "worse than average." Every channel had at least one impairment equal to or worse than the 90-percent point on the nationwide toll connection survey.[2]

The transmitted QAM signals had been generated digitally, with two pseudorandom four-level information symbol streams in quadrature, each repeating after 256 symbols. Each quadrature pair of symbols

therefore conveyed four information bits and the symbol rate was 2400 bauds, making a total bit rate of 9600 bps. The carrier frequency f_c was 1650 Hz, and the double-sideband baseband pulse signal had 12 percent roll-off.

The received signals that were recorded in digital form (12-bit samples, 24-kHz sampling rate) were received from a variety of real and analog-simulated voiceband telephone channels in tandem with an actual 50-km, C2-conditioned, N2-carrier voiceband channel.

As in the simulation of the linear and decision feedback receivers, the adaptive passband signal processors [defined by the set of eqs. (4) and Table I] were preceded by a pair of fixed digital filters that split the incoming signal into in-phase and quadrature components. Each was sampled at time instants $t = \tau + nT$ ($n = 0,1,2,\cdots$). Each simulation was actually of five separate receivers in parallel, with sampling epochs $\tau =$ 0, 0.2T, 0.4T, 0.6T, and 0.8T. The results reported in this paper are in each case for the timing epoch which yielded the best performance. As noted previously in Ref. 9, the decision feedback structure generally produced a relatively small performance spread between the best and the worst timing epochs. The receiver's decisions $\hat{A}(n)$ were formed by quantizing each equalized demodulated output, in-phase or quadrature, into one of the four possible levels $\pm 1, \pm 3$.

Before tabulating the simulation results, we mention some qualitative observations. In the interest of reducing the large numbers of nonlinear coefficients, it would have been desirable that only a few of the observed coefficients be large enough to be significant for all the channels. Unfortunately, this was not the case; no pattern was discernible common to all channels of a significant subset of coefficients; typically, the nonlinear component $Y_{NL}(n)$ in the receiver's output consisted of a large number of small terms, rather than a small number of relatively large terms plus insignificant terms.

Another qualitative observation was that the best values for the adaptation parameters for the nonlinear coefficients were so small that convergence of the nonlinear tap coefficients required at least 2000 symbol intervals, much slower than the convergence rate of the linear coefficients. This is attributed to the high correlation among many of the nonlinear terms. For example, the term $|A_{k_1}|^2 A_{k_2}$ is positively correlated with the linear term A_{k_2}, since $|A_{k_1}|^2$ takes only one of the three possible positive values 2, 10, or 18. Under such circumstances, the $\mathcal{A}$ matrix which describes the correlations among all the terms is expected to have a rather large eigenvalue spread, necessitating small adaptation constants and slow convergence.[13]

During each run, after an initial training period of 2000 symbol intervals to allow the coefficients to converge to nearly stationary values, the simulated receivers switched to a decision-directed mode in which

their decisions $\hat{A}(n)$, right or wrong, were used in the adaptation and decision feedback operations. Since the true transmitted information stream $\{A(n)\}$ was known, the performance was measured by observing the number of decision errors made during 7000 symbol intervals (or 28,000 bits). The empirical probability of the sampled analog error $Y(n) - A(n)$ was also measured, and if no errors were observed during a run, the error probability could be roughly estimated by extrapolating the tail of this distribution, using a computer subroutine by S. B. Weinstein.[14] The tabulated error probability, p_e, is the probability that a four-level symbol is in error; i.e., it is roughly twice the bit error rate. Another tabulated measure of performance was the *output SNR*, defined by

$$\text{output SNR} = \frac{\langle |A(n)|^2 \rangle}{\langle |E(n)|^2 \rangle}$$

where "$\langle \quad \rangle$" denotes the time average.

VII. QUANTITATIVE RESULTS

The simulation results for the NL receiver are tabulated in Table II along with the corresponding results taken from Ref. 9 for the LE and DFE receivers. For each channel, Table II lists the measured impairments and the error probabilities (either observed or extrapolated) for the LE, DFE, and NL receivers. The quantity in parentheses below each error probability is the output SNR in decibels. Error rates below 10^{-5} were extrapolated; in some cases in which the tail of the empirical probability distribution of the quadrature components of $E(n)$ was markedly non-Gaussian, the extrapolation yielded limited accuracy. Figure 4 illustrates the nonlinear compensation for channel 14, which had unusually severe second-harmonic distortion. Figure 4 is plotted on a "probability scale;" i.e., a Gaussian error distribution function would plot as a straight line on it. The distribution function for the linear receiver has distorted tails, indicating the presence of residual nonlinear distortion. However, the curve is nearly straight for the NL receiver, indicating that nonlinear distortion components have been substantially removed.

Comparison of error rates for the three receivers on all the channels is displayed more dramatically by the bar graph of Fig. 5. In all cases, the performance of the NL receiver surpassed that of the other two receivers. (Note that measurable nonlinear distortion was observed on all the channels.) In most cases, the NL receiver afforded a greater improvement in error rate over the DFE receiver than did the DFE receiver over the LE receiver. This is a very significant point. It indicates that if 9600-bps voiceband modems are to be improved by more sophisticated signal processing at the receiver, it is more fruitful to attempt to overcome nonlinear distortion than to concentrate on more sophisticated receiver structures, optimal for linear channel models.

Table II — Experimental comparison of LE, DFE and NL receivers (facility in tandem with Holmdel-Murray Hill N2-carrier line)

		No.5 none	No. 6 Private N Carrier to White Plains	No. 7 Line Simulator	No. 8 Private T1 Carrier to Newark	No. 9 Line Simulator	No. 10 Line Simulator	No. 11 Line Simulator	No. 12 Line Simulator	No. 13 Line Simulator
Measured Impairments	Slope (dB)	0	2	9	4.4	−2	3	11*	11*	0
	Signal-to-noise ratio (dB)	29.0*	22.5†	31	27*	30	35	24.4*	33	34
	Second harmonic (dB)	33.5	28*	33	35	25†	32.1*	28.6*	33.8	34.4
	Third harmonic (dB)	44	31*	22.5†	40	33	47	36.4	49	30.7*
	Phase jitter (peak-to-peak)	<3°	<3°	<3°	<3°	14°† (120 Hz)	17°† (50 Hz)	<3°	<3°	<3°
Error rates (output SNR)	Linear equalization	1×10^{-8} (28.0 dB)	2×10^{-6} (22.4 dB)	6×10^{-3} (17.9 dB)	1×10^{-5} (20.8 dB)	7×10^{-3} (15.0 dB)	8×10^{-6} (23.9 dB)	1×10^{-4} (18.6 dB)	3×10^{-7} (22.6 dB)	3×10^{-6} (23.8 dB)
	Decision feedback equalization	2×10^{-9} (27.8 dB)	4×10^{-6} (22.8 dB)	3×10^{-3} (19.5 dB)	4×10^{-6} (21.2 dB)	9×10^{-3} (15.0 dB)	5×10^{-7} (23.8 dB)	7×10^{-5} (20.2 dB)	7×10^{-10} (24.6 dB)	3×10^{-8} (23.9 dB)
	Nonlinearity equalization	2×10^{-11} (29.4 dB)	1×10^{-6} (24.9 dB)	1×10^{-5} (23.7 dB)	7×10^{-7} (22.3 dB)	2×10^{-4} (18.2 dB)	3×10^{-8} (24.7 dB)	3×10^{-7} (21.7 dB)	3×10^{-12} (28.6 dB)	1×10^{-12} (27.5 dB)

Table II (cont)

		No. 14 Line Simulator	No. 15 Line Simulator	No. 16 Line Simulator	No. 17 Line Simulator	No. 18 DDD Loopback to Dallas	No. 19 (Private T1 Carrier to Newark	No. 20 Private T1 Carrier to Newark	No. 21 Private T1 Carrier to Newark
Measured Impairments	Slope (dB)	0	0	12†	11.1*	7.8	13†	6	8
	Signal-to-noise ratio (dB)	31	31	23†	29*	29*	28*	24.8*	23.2†
	Second harmonic (dB)	20.6†	27.2*	25.2†	32.2*	36.4	31.8*	24.4†	24.6†
	Third harmonic (dB)	49	32*	30.3†	34.7*	32.2*	37	32.6*	28.6†
	Phase jitter (peak-to-peak)	<3°	<3°	15°† (120 Hz)	10°† (120 Hz)	6°	<3°	<3°	<3°
Error Rates (output SNR)	Linear equalization	2×10^{-4} (19.4 dB)	1×10^{-6} (24.5 dB)	1.7×10^{-2} (14.0 dB)	3×10^{-3} (17.4 dB)	1×10^{-3} (18.5 dB)	2.1×10^{-3} (18.3 dB)	5×10^{-4} (18.4 dB)	1.6×10^{-3} (17.8 dB)
	Decision feedback equalization	8×10^{-5} (19.5 dB)	5×10^{-7} (24.5 dB)	3×10^{-2} (14.1 dB)	2×10^{-3} (18.6 dB)	9×10^{-4} (18.3 dB)	2×10^{-3} (19.9 dB)	3×10^{-4} (18.7 dB)	3×10^{-3} (18.0 dB)
	Nonlinearity equalization	2×10^{-9} (26.8 dB)	1×10^{-10} (28.4 dB)	1×10^{-2} (15.6 dB)	3×10^{-5} (20.8 dB)	5×10^{-5} (20.4 dB)	5×10^{-5} (21.6 dB)	3×10^{-5} (20.6 dB)	7×10^{-5} (19.6 dB)

* Indicates worse than 90-percent point in the nationwide toll connection survey.
† Indicates worse than "worst case" 3002 channel impairment limit.

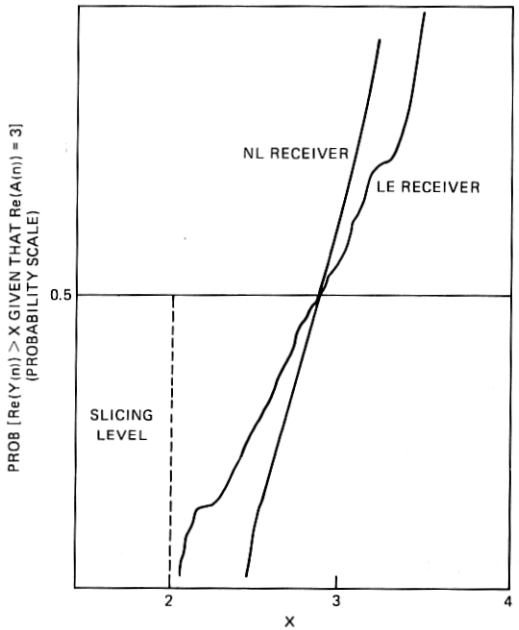

Fig. 4—Comparison of distribution functions of the receiver output $Y(n)$ for the linear and nonlinear receivers (data from channel 14).

Note in Fig. 5 that, for some of the channels, the nonlinearity equalization reduced the error rate by two or three orders of magnitude. However, on other channels, such as 9 and 16* which had most of their impairments in the "severe" category, the error rate was high and the NL receiver afforded very little improvement.

An interesting statistic that can be gleaned from Fig. 5 concerns the ability of the NL receiver to increase the number of channels which yield error rates below a specified maximum. For example, 15 of the 17 channels yield an error rate of better than 10^{-4} with the NL receiver, but only 8 of 17 meet this error rate standard with the LE receiver. For a maximum error rate of 10^{-5}, the number of channels is 10 with the NL receiver and 7 with the LE receiver. For a maximum error rate of 10^{-6}, the numbers of channels are 9 and 3 with the NL and LE receivers, respectively.

The price paid for the better performance of the NL receiver is, of course, its increased complexity, measured by the number of terms comprising $Y_{NL}(n)$ in eq. (4) and its slower convergence. The effect of reducing the number of terms, and therefore the complexity, is treated in the next section.

* Channel 16's impairments, produced by a line simulator, were all "worst case" values.

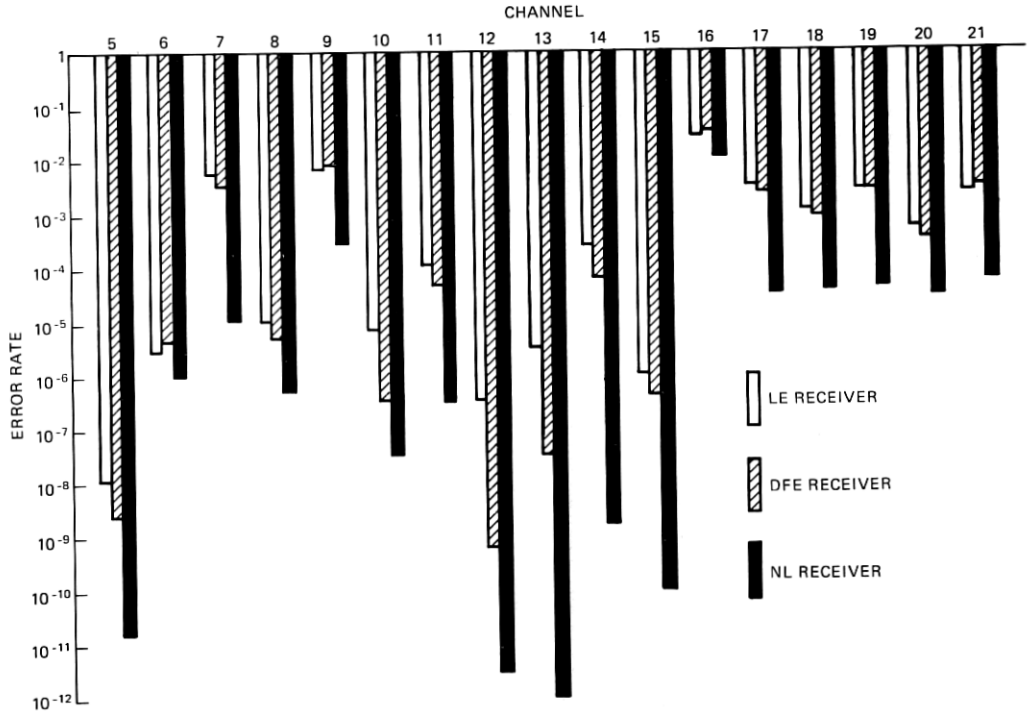

Fig. 5—Comparison of error rates for the three receivers.

VIII. MODIFICATIONS OF THE NONLINEAR RECEIVER STRUCTURE

8.1 Reductions of the number of nonlinear tap coefficients

(*i*) The tap coefficients $\{W^{(12)}_{k_1,k_2,k_3}\}$ and $\{B^{(12)}_{k_1,k_2,k_3}\}$ were set to zero, reducing the total number of nonlinear forward and feedback taps to 37 each. The measured output SNRs for most of the channels were slightly less than those for the full complement of 51 forward and 51 feedback taps, as illustrated in Table III.

(*ii*) A different set of 100 nonlinear terms was created by eliminating all cross-product terms and extending the time span covered by the forward and feedback terms to 10 symbol intervals. Thus, the forward tap coefficients consisted of $\{W^{(0)}_{k,k}\}$, $\{W^{(11)}_{k,k,k}\}$, $\{W^{(12)}_{k,k,k}\}$, $\{W^{(12)}_{k,k}\}$, and $\{W^{(13)}_{k,k,k}\}$, where $-5 \leq k \leq 4$, and the feedback terms consisted of $\{B^{(0)}_{k,k}\}$, $\{B^{(11)}_{k,k,k}\}$, $\{B^{(12)}_{k,k,k}\}$, $\{B^{(2)}_{k,k}\}$, and $\{B^{(3)}_{k,k,k}\}$, where $1 \leq k \leq 10$. Some resulting output SNRs are tabulated in part (*iii*) following.

(*iii*) A smaller set of nonlinear taps was created by taking a subset of 46 of the original set of 102 nonlinear taps. The resulting output SNRs for several channels are shown in Table IV, along with the corresponding set of SNRs from the original NL receiver structure with 102 nonlinear taps and also from the receiver with 100 nonlinear taps, described in item (*ii*), above.

The results of items (*i*), (*ii*), and (*iii*), compared with the original results using the NL receiver with 102 nonlinear tap coefficients indicate that a large number of nonlinear correction terms is necessary to yield substantial performance improvement. Undoubtedly, still better performance would have been attained by using more than 102 nonlinear taps. The results of item (*ii*) also showed that elimination of the cross-product terms degraded performance, even though the remaining nonlinear terms encompassed a longer time span.

Table III — Output SNR (dB) for nonlinear receivers

Channel	102 nonlinear taps	74 nonlinear taps
5	29.4	29.4
6	24.9	23.8
7	23.7	22.7
8	22.3	22.1
9	18.2	17.5
10	24.7	24.5
11	21.7	21.5
12	28.6	27.5

Table IV — Output SNR (dB) for nonlinear receivers

Channel	Original (102 Taps)	(*ii*) 100 Taps	(*iii*) 46 Taps
9	18.2	17.7	17.5
13	27.5	25.8	25.7
14	26.8	23.7	23.0
15	28.4	25.6	26.5

(*iv*) The number of nonlinear taps was also reduced to 46 by eliminating all coefficients $\{W^{(2)}_{k1,k2}\}$, $\{B^{(2)}_{k1,k2}\}$, $\{W^{(3)}_{k1,k2,k3}\}$, and $\{B^{(3)}_{k1,k2,k3}\}$. The resulting output SNR on channel 14 was only 21.3 dB, as compared to 24.8 dB for 102 nonlinear taps. Thus, it appears that at least the last four sets of coefficients (associated with second and third harmonics of the carrier frequency) are significant and should be retained.

8.2 A variation in the receiver structure tested for channel 20

The forward nonlinear tap coefficients weight various quadratic and cubic products of the sampled received signals. One might speculate that if *linear* distortion were removed from the received samples before their nonlinear processing, the nonlinear distortion remaining in the output might be further reduced. Accordingly, we simulated an NL receiver structure which was the same as that shown in Fig. 4 except that there are no linear feedback taps and the input to the forward nonlinear taps comes from the output of the linear forward taps instead of directly from the phase splitter. Since the adaptive linear forward taps, constituting the passband equilizer, are in tandem with the adaptive nonlinear taps in this structure, the mean squared error is not a convex function of the nonlinear tap coefficients, and hence the question of convergence is more complicated. Nevertheless, this structure was simulated on channel 20. The resulting output SNR was 20.0 dB compared to the 20.6 dB obtained from the original receiver structure. Thus, prior linear equalization did not appear preferable.

IX. CONCLUSIONS

The simulations have demonstrated that nonlinearity-equalizing QAM receivers can provide substantially better performance than can conventional linear or decision feedback equalization receivers over a variety of voiceband telephone channels. This encouraging result may stimulate further research aimed at finding less complicated receiver structures for overcoming channel nonlinearities.

The number of nonlinear terms that can be considered for inclusion in the NL receiver's analog output $Y(n)$ is potentially enormous. For example, the number of different terms $R(k_1)R(k_2)R(k_3)^*$ for all indices k_1, k_2 and k_3 between $-N$ and $+N$ is $(2N+1)^2(N+1)$, which is much more than $(2N+1)$, the corresponding number of linear terms $\{R(k)\}$ in that range of indices. The simulation results indicated that inclusion of a large number of nonlinear terms, including "cross-product" terms for which $k_1 \neq k_2 \neq k_3$, may be necessary. Reductions in the number of terms and a variation of the NL receiver's structure, in which adaptive linear processing preceded nonlinear processing, resulted in worsened performance.

Perhaps the major conclusion to be drawn concerns means for im-

proving the reliability of high-speed data transmission over the population of voiceband telephone channels. The simulations reported in Ref. 9 showed that decision feedback equalization, which is known theoretically to be superior to linear equalization in overcoming severe linear distortion, only moderately bettered the error rate obtained with linear equalization, especially on voiceband channels meeting C2 conditioning standards. However, the results summarized by Fig. 5 indicated that there is more to be gained by mitigating nonlinear distortion than in using more elaborate methods (beyond linear or decision feedback equalization) of mitigating linear distortion.

APPENDIX

In this appendix, we derive the form of the analytic signal that emerges from the summed filtered outputs of the quadratic and cubic nonlinearities. The real and imaginary parts of this analytic signal will then be the in-phase and quadrature components, respectively, of the nonlinearly distorted received QAM signal. The following theorems, proven in Ref. 11, will be required:

Theorem 1: *Given real waveforms* $u(t)$ *and* $v(t)$, *defined on* $-\infty < t < \infty$ *with respective Hilbert transforms* $\check{u}(t)$ *and* $\check{v}(t)$, *the convolution*

$$w(t) = \int_{-\infty}^{\infty} v(\tau)u(t-\tau)d\tau \tag{7}$$

has Hilbert transform

$$\check{w}(t) = \int_{-\infty}^{\infty} \check{v}(\tau)u(t-\tau)d\tau = \int_{-\infty}^{\infty} v(\tau)\check{u}(t-\tau)d\tau. \tag{8}$$

Thus, if $v(t)$ is the input to a filter whose impulse response is $u(t)$, the analytic output signal is

$$w(t) + j\check{w}(t) = \int_{-\infty}^{\infty} (v(\tau) + j\check{v}(\tau))u(t-\tau)d\tau$$

$$= \int_{-\infty}^{\infty} v(\tau)(u(t-\tau) + j\check{u}(t-\tau))d\tau. \tag{9}$$

Theorem 2: *The analytic signal resulting from the convolution can also be expressed as*

$$w(t) + j\check{w}(t) = \frac{1}{2}\int_{-\infty}^{\infty} (v(\tau) + j\check{v}(\tau))(u(t-\tau) + j\check{u}(t-\tau))d\tau. \tag{10}$$

Now we consider an analytic signal of the form

$$X(t) = e^{j2\pi f_c t}\sum_n A(n)F(t-nT), \tag{11}$$

as in expression (2) of the text. The squaring and cubing elements in Fig. 2 operate on $x(t)$, the real part of $X(t)$. The response of the squaring element to $\mathrm{Re}(X(t))$ can be written

$$x(t)^2 = \frac{1}{2}\mathrm{Re}\left[e^{j4\pi f_c t}\sum_{n_1,n_2} A(n_1)A(n_2)F(t-n_1T)F(t-n_2T)\right] + \frac{1}{2}\left[\sum_{n_1,n_2} A(n_1)A(n_2)^*F(t-n_1T)F(t-n_2T)^*\right]. \quad (12)$$

Of the complex expressions in square brackets in (12), the first is complex and analytic, since it is the square of an analytic signal (its spectrum is nonzero only for positive frequencies). Thus, from Theorem 2, the analytic signal that results from passing the first part of expression (12) through a passband filter 2 is of the form

$$U_2(t) = e^{j4\pi f_c t}\sum_{n_1}\sum_{n_2} A(n_1)A(n_2)G_2(t-n_1T,t-n_2T), \quad (13)$$

where $G_2(t-n_1T,t-n_2T)e^{j4\pi f_c t}$ is a complex analytic waveform, whose spectrum has been limited by filter 2 to $0 < f < 2f_c$. The second term in (12) is baseband, real, and not analytic.† However, from Theorem 1, the analytic signal resulting from passing the second term through filter 2 has the form

$$U_0(t) = \sum_{n_1,n_2} A(n_1)A(n_2)^*G_0(t-n_1T,t-n_2T), \quad (14)$$

where $G_0(t-n_1T,t-n_2T)$ is an analytic waveform, whose spectrum is confined to $0 < f < 2f_c$.

The cubic nonlinear terms are handled similarly. The cube of the input signal $\mathrm{Re}(X(t))$ can be written

$$x(t)^3 = \frac{1}{4}\mathrm{Re}\left[e^{j6\pi f_c t}\sum_{n_1,n_2,n_3} A(n_1)A(n_2)A(n_3)F(t-n_1T)\cdot F(t-n_2T)F(t-n_3T)\right] + \frac{3}{8}e^{j2\pi f_c t}\sum_{n_1,n_2,n_3} A(n_1)A(n_2)A(n_3)^*F(t-n_1T)F(t-n_2T)\cdot F(t-n_3T)^* + \frac{3}{8}e^{-j2\pi f_c t}\sum_{n_1,n_2,n_3} A(n_1)^*A(n_2)^*A(n_3)\cdot F(t-n_1T)^*F(t-n_2T)^*F(n-n_3T). \quad (15)$$

The first term in square brackets (15) is analytic, being the cube of an analytic signal. The other two terms in (15) are not analytic, since their

† The ranges of the indices n_1 and n_2 in (12) and (13) are assumed to be the same.

Fourier transforms are not necessarily zero for negative frequencies. The analytic signal resulting from passing $x(t)^3$ through bandpass filter 3 can be written by applying Theorem 2 to the first term of (15) and Theorem 1 to the second and third terms. The resulting analytic signal is the sum of three analytic signals, $U_3(t)$, $U_{11}(t)$, and $U_{12}(t)$, which have the following forms:

$$U_3(t) = e^{j6\pi f_c t} \sum_{n_1,n_2,n_3} A(n_1)A(n_2)A(n_3) \cdot G_3(t - n_1T, t - n_2T, t - n_3T). \quad (16)$$

$$U_{11}(t) = e^{j2\pi f_c t} \sum_{n_1,n_2,n_3} A(n_1)A(n_2)A(n_3)^* \cdot G_{11}(t - n_1T, t - n_2T, t - n_3T). \quad (17)$$

$$U_{12}(t) = e^{-j2\pi f_c t} \sum_{n_1,n_2,n_3} A(n_1)^*A(n_2)^*A(n_3) \cdot G_{12}(t - n_1T, t - n_2T, t - n_3T). \quad (18)$$

The $G(\ )$ signals are complex, and the spectra of the analytic signals $U_3(t)$, $U_{11}(t)$, and $U_{12}(t)$ are all confined to the range $0 < f < 2f_c$ by bandpass filter 3.

REFERENCES

1. R. W. Lucky, "Modulation and Detection for Data Transmission on the Telephone Channel," in *New Directions in Signal Processing in Communication and Control*, ed. by J. K. Skwirzynski, Leyden: Noordhoff, 1975, pp. 321–327.
2. F. P. Duffy and T. W. Thatcher, Jr., "Analog Transmission Performance on the Switched Telecommunications Network," B.S.T.J., *50*, No. 4 (April 1971), pp. 1311–1347.
3. R. R. Anderson and D. D. Falconer, "Modem Evaluation on Real Channels Using Computer Simulation," Proc. National Telecomm. Conf., Dec. 1974, San Diego, pp. 877–883.
4. S. Benedetto, E. Biglieri, and R. Daffara, "Performance of Multilevel Baseband Digital Systems in a Nonlinear Environment," IEEE Trans. Comm., *COM-24*, No. 10 (October 1976), pp. 1166–1175.
5. W. J. Lawless and M. Schwartz, "Binary Signaling over Channels Containing Quadratic Nonlinearities," IEEE Trans. Comm., *COM-22*, No. 2 (March 1974), pp. 288–298.
6. N. Wiener, *Nonlinear Problems in Random Theory*, Cambridge, Mass.: M.I.T. Press and J. Wiley, 1958.
7. T. Arbuckle, "Nonlinear Equalization System Including Self- and Cross-Multiplication of Sampled Signals," U.S. Patent 3,600,681, Aug. 17, 1971.
8. E. J. Thomas, "Some Considerations on the Application of the Volterra Representation of Nonlinear Networks to Adaptive Echo Cancellers," B.S.T.J., *50*, No. 8 (October 1971), pp. 2797–2805.
9. D. D. Falconer, "Application of Passband Decision Feedback Equalization in Two-Dimensional Data Communications Systems," IEEE Trans. Comm., *COM-24*, No. 10 (October 1976), pp. 1159–1166.
10. D. D. Falconer, "Jointly Adaptive Equalization and Carrier Recovery in Two Dimensional Digital Communication Systems," B.S.T.J., *55*, No. 3 (March 1976), pp. 317–334.
11. J. Dungundji, "Envelopes and Pre-Envelopes of Real Waveforms," IRE Trans. on Info. Theory, Sept. 1957, pp. 53–57.
12. R. D. Gitlin, E. Y. Ho, and J. E. Mazo, "Passband Equalization for Differentially Phase Modulated Data Signals," B.S.T.J., *52*, No. 2 (February 1973), pp. 219–238.

13. A. Gersho, "Adaptive Equalization of Highly Dispersive Channels for Data Transmission," B.S.T.J., *48*, No. 1 (January 1969), pp. 55–70.
14. S. B. Weinstein, "Theory and Applications of Some Classical and Generalized Asymptotic Distributions of Extreme Values," IEEE Trans. Inform. Theory, *IT-19*, No. 2 (March 1973), pp. 148–154.